Journal of Alloys and Compounds 509 (2011) 3208–3210

Contents lists available at ScienceDirect

Journal of Alloys and Compounds

journal homepage: www.elsevier.com/locate/jallcom

Crystal structure and magnetic behavior of novel R_2PdIn_8 (R = Pr, Nd, and Sm) compounds

D. Kaczorowski[a,*], B. Belan[b], L. Sojka[b], Ya. Kalychak[b,**]

[a] Institute of Low Temperature and Structure Research, Polish Academy of Sciences, P. O. Box 1410, 50-950 Wrocław 2, Poland
[b] Faculty of Chemistry, Ivan Franko National University of Lviv, Kyryla i Mefodiya St. 6, UA-79005 Lviv, Ukraine

ARTICLE INFO

Article history:
Received 12 October 2010
Received in revised form
10 November 2010
Accepted 11 November 2010
Available online 14 December 2010

Keywords:
Rare-earth intermetallics
Indides
Crystal structure
Magnetic properties

ABSTRACT

A new series of R_2PdIn_8 intermetallics, where R = Pr, Nd, and Sm, was prepared by arc-melting the constituents under argon atmosphere and studied by means of X-ray diffraction and magnetic measurements. The compounds crystallize with a tetragonal structure of the Ho_2CoGa_8 type (space group *P*4/*mmm*). At very low temperatures, they order antiferromagnetically, and the Nd-based indide presumably exhibits an additional magnetic phase transition in the ordered region.

1. Introduction

A family of Ce_2TIn_8 intermetallics with T = Co, Rh and Ir [1], which crystallize with a tetragonal structure of the Ho_2CoGa_8 type (space group *P*4/*mmm*) [2], have attracted much attention due to their intriguing physical properties, like heavy-fermion ambient-pressure superconductivity in Ce_2CoIn_8 [3] and interplay of pressure-induced superconductivity and antiferromagnetism in Ce_2RhIn_8 [4]. Recently we reported on the formation of another representative of the Ce_2TIn_8 series with T = Pd [5]. The magnetic, electrical transport and thermodynamic properties of the new compound were studied in wide ranges of temperature and magnetic field strength. The results revealed Ce_2PdIn_8 to be a paramagnetic Kondo lattice down to $T_c = 0.7$ K below which temperature it becomes superconducting [6,7]. The characteristic parameters of its electronic ground state clearly reflect heavy-fermion nature of the observed superconductivity that is likely driven by magnetic fluctuations at the verge of a quantum phase transition.

In order to understand the role of magnetic anisotropy and crystal field effect on the properties of the Ce_2TIn_8 (T = Co, Rh and Ir) compounds, a few studies have been carried out on isostructural systems in which Ce is replaced by different rare-earth atom R [8–10]. For similar reason, we have undertaken investigations of the phases R_2PdIn_8 that could be counterparts to Ce_2PdIn_8, very useful for interpretation of the anomalous behavior of the latter compound. In this paper, we report for the first time on the formation and the magnetic properties of the compounds with R = Pr, Nd, and Sm.

2. Experimental

Polycrystalline samples of Pr_2PdIn_8, Nd_2PdIn_8 and Sm_2PdIn_8 were synthesized by arc-melting stoichiometric amounts of the constituents [purity: lanthanides 99.9 wt.% (Johnson-Matthey), palladium 99.99 wt.% (Chempur), indium 99.99 wt.% (Johnson-Matthey)] under titanium-gettered argon atmosphere. The ingots were turned over and remelted several times to ensure homogeneity. Weight losses during the arc-melting were smaller than 0.5 wt%. Subsequently, the samples were wrapped with tantalum foil, sealed in quartz tubes and annealed at 600 °C for 1 month.

Quality of the products was checked by X-ray powder diffraction using a HZG-4a powder diffractometer with Cu $K\alpha_1$ radiation. For each sample a few minor foreign Bragg peaks were observed due to tiny contamination by indium. The crystal structure of the main phases was determined using a Rietveld type refinement program DBWS [11].

Magnetic measurements were performed in the temperature range of 1.71–300 K and in applied magnetic fields up to 5 T employing a commercial superconducting quantum interference device (SQUID) magnetometer.

3. Results and discussion

3.1. Crystal structures

The X-ray powder diffraction examinations revealed that all three compounds studied crystallize with a tetragonal structure of the Ho_2CoGa_8 type (space group *P*4/*mmm*, No. 123) [2]. In the unit cells of R_2PdIn_8, the rare-earth atoms occupy the 2*g* (0 0 z_R)

* Corresponding author. Tel.: +48 71 34 350 21; fax: +48 71 34 410 19.
** Corresponding author.
E-mail addresses: D.Kaczorowski@int.pan.wroc.pl (D. Kaczorowski), Kalychak@franko.lviv.ua (Ya. Kalychak).

0925-8388/$ – see front matter © 2010 Elsevier B.V. All rights reserved.
doi:10.1016/j.jallcom.2010.11.207

Table 1
Crystallographic data for the R_2PdIn_8 compounds.

Compound	Pr_2PdIn_8	Nd_2PdIn_8	Sm_2PdIn_8
Content[a] (mol%)	98.6(1)	97.6(1)	92.3(1)
Lattice parameters			
a (Å)	4.6715(2)	4.6712(3)	4.6510(2)
c (Å)	12.1354(6)	12.1341(8)	12.0644(8)
Unit cell volume, V (Å^3)	264.83(2)	264.77(3)	260.97(3)
Density, D_X (g/cm^{-3})	8.197	8.240	8.439
Texture parameter, G [direction]	0.933(4) [0 0 1]	0.939(5) [0 0 1]	0.940(4) [0 0 1]
Reliability factors			
R_p	0.0326	0.0531	0.0291
R_{wp}	0.0415	0.0744	0.0370
R_B	0.1061	0.1342	0.1237
Zero value, 2θ (°)	−0.046(2)	−0.0186(3)	−0.090(3)
Mixing parameter, μ	0.78(1)	0.98(2)	0.85(1)
Reflections number	411	386	409
Positional parameters			
z_R	0.3097(5)	0.3097(7)	0.3097(7)
z_{In1}	0.1237(3)	0.1244(3)	0.1248(3)
z_{In3}	0.3060(6)	0.3043(7)	0.3064(7)

[a] For each sample an admixture of free indium metal was observed in the amount of 1.4(1), 2.4(1) and 7.7(1) mol% in Pr_2PdIn_8, Nd_2PdIn_8 and Sm_2PdIn_8, respectively.

sites, the palladium atoms are located at the 1*a* (0 0 0) sites, while the indium atoms are distributed over three inequivalent crystallographic sites: 4*i* (0 ½ z_{In1}), 2*e* (0 ½ ½), and 2*h* (½ ½ z_{In3}). The refined values of the lattice and free positional parameters are listed in Table 1, together with some details on the crystal structure refinements performed.

The R_2PdIn_8 compounds belong to a homologous series $R_mPd_nIn_{3m+2n}$, which is based on RIn_3 ($AuCu_3$-type) and $PdIn_2$ ($PtHg_2$-type) slabs (see Fig. 1), assembled in the unit cell with the amount m and n, respectively. The coordination polyhedra of the R atoms are cubooctahedra formed by indium atoms (coordination number CN = 12). The Pd atoms are surrounded by indium atoms

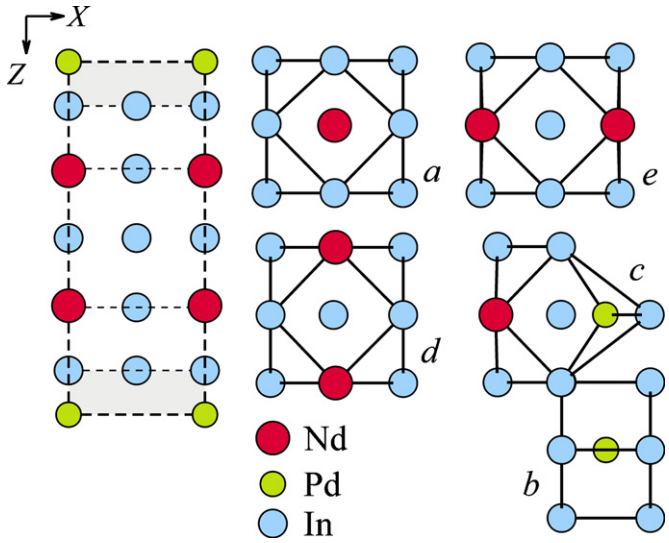

Fig. 1. Unit cell of Nd_2PdIn_8 projected onto the *XZ* plane and the coordination polyhedra of all the atoms: Nd (a), Pd (b), In1 (c), In2 (d) and In3 (e). $NdPd_3$ ($AuCu_3$-structure type) and $PdIn_2$ ($PtHg_2$-structure type) slabs are marked transparent and light grey, respectively.

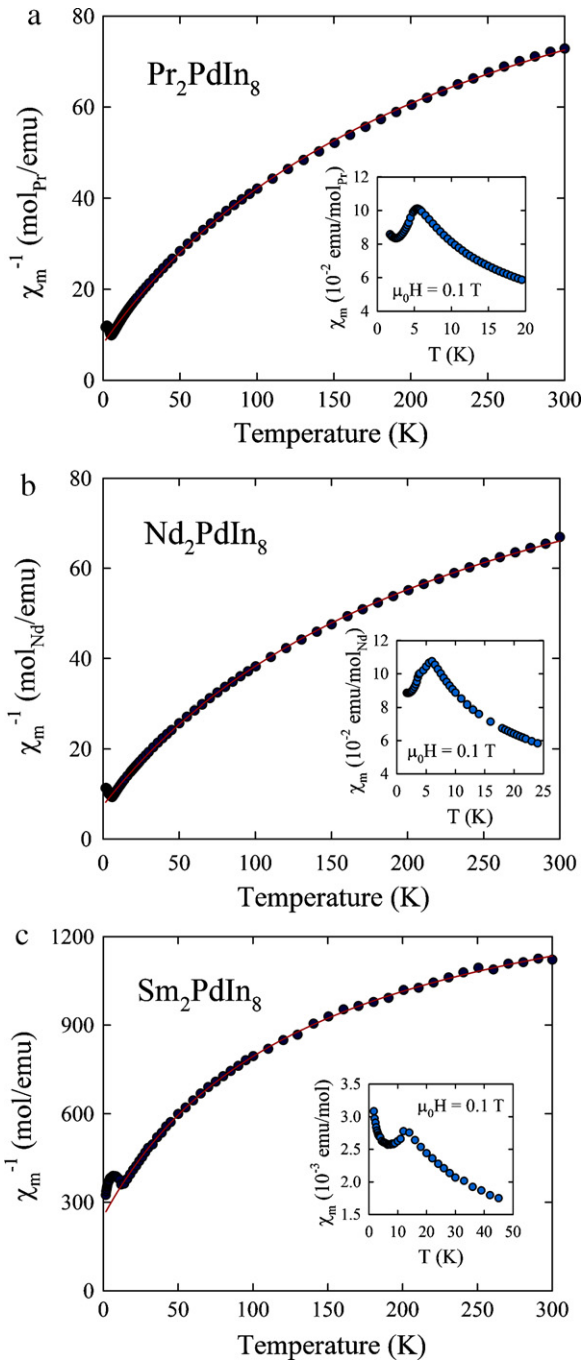

Fig. 2. Temperature dependencies of the inverse molar magnetic susceptibility of Pr_2PdIn_8 (a), Nd_2PdIn_8 (b) and Sm_2PdIn_8 (c) measured in a field of 0.1 T. The solid lines represent the modified Curie–Weiss fits discussed in the text. The insets show the molar magnetic susceptibility at low temperatures.

arranged into cubes (CN = 8). In turn, the In2 and In2 atoms are located inside cubooctahedra formed by In and *R* atoms (CN = 12), while the coordination sphere of the In1 atoms is a deformed cubooctahedron (CN = 11). The main interatomic distances are listed in Table 2. All of them are somewhat smaller than or close to the sums of the respective atomic radii [12].

3.2. Magnetic properties

The temperature dependencies of the inverse molar magnetic susceptibility of Pr_2PdIn_8, Nd_2PdIn_8 and Sm_2PdIn_8 are displayed in Fig. 2. As marked by the solid lines, in extended temperature

Table 2
Interatomic distances (Å) in the unit cells of the R_2PdIn_8 compounds.

Pr_2PdIn_8				Nd_2PdIn_8				Sm_2PdIn_8			
Pr	In1	3.263(6)	4×	Nd	In1	3.230(6)	4×	Sm	In1	3.231(6)	4×
	In2	3.282(5)	4×		In2	3.290(5)	4×		In2	3.264(5)	4×
	In3	3.304(0)	4×		In3	3.304(0)	4×		In3	3.289(0)	4×
Pd	In1	2.767(3)	8×	Pd	In1	2.786(2)	8×	Pd	In1	2.767(3)	8×
In1	Pd	2.767(3)	2×	In1	Pd	2.786(2)	2×	In1	Pd	2.767(3)	2×
	In1	2.966(7)	1×		In1	3.036(5)	1×		In1	2.999(7)	1×
	In3	3.223(7)	2×		In3	3.186(6)	2×		In3	3.191(7)	2×
	Pr	3.263(6)	2×		Nd	3.230(6)	2×		Sm	3.231(6)	2×
	In1	3.303(0)	4×		In1	3.303(0)	4×		In1	3.289(0)	4×
In2	Pr	3.282(5)	4×	In2	Nd	3.290(5)	4×	In2	Sm	3.264(5)	4×
	In2	3.303(0)	4×		In2	3.303(0)	4×		In2	3.289(0)	4×
	In3	3.323(6)	4×		In3	3.336(6)	4×		In3	3.305(6)	4×
In3	In1	3.223(7)	4×	In3	In1	3.186(6)	4×	In3	In1	3.191(7)	4×
	Pr	3.304(0)	4×		Nd	3.304(0)	4×		Sm	3.289(0)	4×
	In2	3.323(6)	4×		In2	3.336(6)	4×		In2	3.305(6)	4×

intervals, the experimental data can be well described by the so-called modified Curie–Weiss law $\chi(T) = \chi_0 + C/(T - \theta_p)$. From the presented least-squares fits, the effective magnetic moment, calculated as $\mu_{eff} = \sqrt{8C}$, is derived as being equal to 3.81(6) μ_B in Pr_2PdIn_8, 4.01(5) μ_B in Nd_2PdIn_8 and 0.77(6) μ_B in Sm_2PdIn_8. These values are somewhat different from those expected within the Russell–Saunders coupling scenario for the respective trivalent rare-earth ions (3.58, 3.62 and 0.84 μ_B, respectively [13]). The inverse magnetic susceptibility of the three ternaries are strongly curvilinear functions of the temperature, which is accounted for by large values of the temperature independent term being $\chi_0 = 8.0(3) \times 10^{-3}$ emu/mol, $\chi_0 = 8.8(2) \times 10^{-3}$ emu/mol and $\chi_0 = 6.5(8) \times 10^{-4}$ emu/mol, for the Pr-, Nd- and Sm-based indide, respectively. Whereas the behavior found in the latter phase can be attributed to the closeness in energy of the terms $^6H_{5/2}$ and $^6H_{7/2}$ that originate from the Sm^{3+} ground multiplet [13], such a strong curvature of $\chi^{-1}(T)$ seen for the other two compounds seems rather unusual for rare-earth-based materials with stable 4*f* shell, and probably results from exceptionally large crystalline electric field splittings.

For all the R_2PdIn_8 phases studied, the derived paramagnetic Curie temperature θ_p is negative ($\theta_p = -15.7(7)$, $-16.1(6)$, $-18.9(9)$ K, for Pr_2PdIn_8, Nd_2PdIn_8 and Sm_2PdIn_8, respectively). This feature might manifest antiferromagnetic correlations, and thus long-range magnetic ordering could be expected to occur at low temperatures. Indeed, as displayed in the insets to the main panels in Fig. 2, the magnetic susceptibility curves of Pr_2PdIn_8, Nd_2PdIn_8 and Sm_2PdIn_8 form pronounced characteristic maxima, which manifest the onsets of the antiferromagnetic state below $T_N = 5.2(2)$, 5.9(1) and 12.5(2) K, respectively. In addition, $\chi(T)$ of the Nd-based compound exhibits a distinct kink at 3.5(2) K that likely marks a subsequent order-order phase transition, e.g. a change in the magnetic structure. Furthermore, for all three compounds investigated, the magnetic susceptibility makes an upturn at the lowest temperatures that may hint at some rearrangement of the magnetic moments deeply in the ordered region. To clarify all these magnetic features neutron diffraction experiments are indispensable.

Fig. 3 presents the magnetization isotherms of Pr_2PdIn_8, Nd_2PdIn_8 and Sm_2PdIn_8, taken at 1.71 K. For the two former compounds, $\sigma(H)$ exhibits a clear inflection near 2 T and 1.5 T, respectively, which is reminiscent of metamagnetic-like transitions, and hence it corroborates antiferromagnetic nature of the electronic ground states in these ternaries. In the case of Sm_2PdIn_8 no such magnetization anomaly is obvious, yet the observed straight-line behavior of $\sigma(H)$ is also compatible with antiferromagnetism.

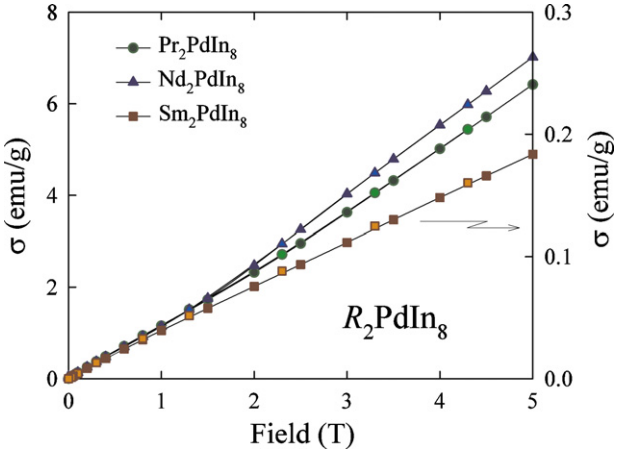

Fig. 3. Field variations of the magnetization in Pr_2PdIn_8, Nd_2PdIn_8 and Sm_2PdIn_8 (note different vertical scale), measured at 1.71 K with increasing (dark-colored symbols) and decreasing (light-colored symbols) field strength.

References

[1] Ya.M. Kalychak, V.I. Zaremba, R. Pöttgen, M. Lukachuk, R.-D. Hoffmann, in: K.A. Gschneider Jr., V.K. Pecharsky, J.-C. Bünzli (Eds.), Handbook on the Physics and Chemistry of Rare Earths, vol. 34, Elsevier, Amsterdam, 2005 (Chapt. 218).
[2] Yu.M. Grin, Ya.P. Yarmolyuk, E.I. Gladyshevskii, Kristallografiya 24 (242) (1979) (in Russian).
[3] G. Chen, S. Ohara, M. Hedo, Y. Uwatoko, K. Saito, M. Sorai, I. Sakamoto, J. Phys. Soc. Jpn. 71 (2002) 2836.
[4] M. Nicklas, V.A. Sidorov, H.A. Borges, P.G. Pagliuso, C. Petrovic, Z. Fisk, J.L. Sarrao, J.D. Thompson, Phys. Rev. B 67 (2003) 020506(R).
[5] D. Kaczorowski, A.P. Pikul, B. Belan, L. Sojka, Ya. Kalychak, Physica B 404 (2009) 2975.
[6] D. Kaczorowski, A.P. Pikul, D. Gnida, V.H. Tran, Phys. Rev. Lett. 103 (2009) 027003;
D. Kaczorowski, A.P. Pikul, D. Gnida, V.H. Tran, Phys. Rev. Lett. 104 (2010) 059702.
[7] D. Kaczorowski, D. Gnida, A.P. Pikul, V.H. Tran, Solid State Commun. 150 (2010) 411.
[8] P.G. Pagliuso, D.J. Garcia, E. Miranda, E. Granado, R. Lora Serrano, C. Giles, J.G.S. Duque, R.R. Urbano, C. Rettori, J. Appl. Phys. 99 (2006) 08P703.
[9] R. Lora-Serrano, L. Mendonça Ferreira, D.J. Garcia, E. Miranda, C. Giles, J.G.S. Duque, E. Granado, P.G. Pagliuso, Physica B 384 (2006) 326.
[10] C. Adriano, R. Lora-Serrano, C. Giles, F. de Bergevin, J.C. Lang, G. Srajer, C. Mazzoli, L. Paolasini, P.G. Pagliuso, Phys. Rev. B 76 (2007) 104515.
[11] D.B. Wiles, A. Sakthivel, R.A. Young, Program DBW3.2s for Rietveld Analysis of X-ray and Neutron Powder Diffraction Patterns, version 9411.PC, Georgia Institute of Technology, Atlanta, 1995.
[12] J. Emsley, The Elements, Clarendon Press, Oxford, 1991.
[13] K.N.R. Taylor, M.I. Darby, Physics of Rare Earth Solids, Chapman & Hall, London, 1972.